ADSORPTION OF Fe^{2+}, Pb^{2+}, Zn^{2+} AND Cr^{6+} IONS FROM AQUEOUS SOLUTIONS USING NATURAL, AMMONIUM OXALATE AND SODIUM HYDROXIDE MODIFIED KAOLINITE CLAY

Lawal, J.A.[1], *Odebunmi, E.O.[1] and Adekola, F.A.[2]

[1]Department of Chemistry, University of Ilorin, Nigeria
[2]Department of Industrial Chemistry, University of Ilorin, Nigeria
jonnylawal@gmail.com; eodebunmi@unilorin.edu.ng; fadekola@unilorin.edu.ng
*Corresponding author: eodebunmi@unilorin.edu.ng; +2348035951353
(Received: 20th May, 2020; Accepted: 15th September, 2020)

ABSTRACT

In this paper, Fe^{2+}, Pb^{2+}, Zn^{2+} and Cr^{6+} ions removal from contaminated water with natural Nigerian kaolinite clay (AK-clay), and that removed with kaolinite clay modified with either ammonium oxalate (AK-AO) or sodium hydroxide (AK-S) were presented. The clay was characterized using X-Ray Diffractometry (XRD), Fourier Transform Infrared Spectroscopy (FTIR), Scanning Electron Microscopy (SEM) and Brunanuer-Emmett-Teller (BET) method. The parameters investigated include pH, adsorbent particle size, shaking speed, metal ion concentration and temperature. The optimum conditions were applied to the modified samples. Design-expert software was used to design the experimental conditions using Response Surface Methodology (RSM). The mineralogical characterization showed the purified 63 μm fraction of the clay as kaolin. Analysis of Variance shows the adsorption of the metal ions was statistically significant with p-valves > 0.0001 at 95 % confidence limit. Pseudo second-order kinetic model was found to fit the adsorption data for all the metal ions. The adsorption of Fe^{2+}, Pb^{2+} and Cr^{6+} ions was best described by the Langmuir isotherm model, while Freundlich isotherm model best fitted the adsorption data for Zn^{2+} ion. Thermodynamic analysis of adsorption data shows the metal ions adsorption was spontaneous, endothermic and accompanied by positive entropy change. Compared to unmodified natural clay, AK-S clay increased adsorption capacity for Fe^{2+}, Pb^{2+}, Zn^{2+} and Cr^{6+} ions from 14.1 to 18.425 mg/g, 18.4 to 19.8 mg/g, 16.875 to 19.9 mg/g and 7.65 to 8.15 mg/g respectively. The AK-AO clay increased the uptake of Fe^{2+} ion from 14.1 to 17.35 mg/g with a slight increase for Zn^{2+} ion (16.875 to 16.95 mg/g). The adsorption capacity of AK-clay for all the metal ions was enhanced by NaOH modification while the ammonium oxalate modification significantly enhanced the adsorption capacity only for Fe^{2+} ion. The results show that NaOH and ammonium oxalate modified kaolinite clay are effective for remediation of heavy metal-laden wastewater.

Keywords: Kaolinite, metal ions, adsorption, kinetics, adsorption isotherm

INTRODUCTION

Effluents discharge from industries is a major source of environmental pollution globally. Heavy metals are one of the dominant contaminants in industrial effluents and discharging heavy-metal laden contaminated wastewater into water bodies at elevated concentrations is considered lethal to living organisms. Excessive accumulation of metal ions in living tissue impedes the biological functions of vital organs resulting into health problems (Chandra and Mandal, 2000; Jiang *et al.*, 2010).

Several treatment methods have been devised for removal of heavy metals from wastewater. Adsorption technique is considered one of the effective low-cost methods for removal of heavy metals. Adsorption of heavy metals from aqueous solutions has been studied using different adsorbents including clay (Sari *et al.*, 2007; Adebowale *et al.*, 2008; Dawodu and Akpomie, 2014). The use of kaolinite clay for adsorption is worthwhile because of its abundance in deposit especially in Nigeria (Olusola *et al.*, 2011; Fakoluji *et al.*, 2012). Kaolinite clay is a phyllosilicate clay mineral of interlayer structure type 1:1 with ideal structural formula of $Al_2Si_2O_5(OH)_4$ (Barth, 1994; Bergaya *et al.*, 2006; Uddin, 2017). Several researchers have investigated the adsorption of heavy metal ions in aqueous solution on kaolinite clay. The data obtained from adsorption of Pb^{2+}, Cu^{2+}, Fe^{3+}, Mn^{2+} and Zn^{2+} ions on kaolinite showed that there was favourable adsorption of the metal ions (Kamel *et al.*, 2004). Investigation of adsorption of Pb^{2+}, Cu^{2+}, Cd^{2+}, and Zn^{2+} ions on different clays have shown that Pb^{2+} ion, has greater affinity for the clays than the other metal ions (Olaofe *et al.*, 2015). Nigerian kaolinite clay

have been used to simultaneous adsorb Ni^{2+} and Mn^{2+} ions from wastewater (Dawodu and Akpomie, 2014).

To improve the adsorption capacity of clay adsorbents, several reagents such as inorganic and organic acids, alkaline and organic salts have been used to activate or modify them. Acid treatment of clay minerals helps to remove impurities and increase silica to alumina ratio and surface area (Al-Harahsheh *et al*., 2009; Emam *et al*., 2016). Modification with alkaline compound especially NaOH has been found to increase the exchangeable ion content and increase the negative charge sites (Al-Harahsheh *et al*., 2009; Uddin, 2017). Treatment with organic compounds containing functional groups and non-functional organic cations has also been reported to enhance adsorption capacities of clays especially by complexing with metal ions (Krishna *et al*., 2001; Cruz-Guzman *et al*., 2006; Lee and Tiwari, 2012).

In this study, the adsorption of aqueous solutions of Fe^{2+}, Pb^{2+}, Zn^{2+} and Cr^{6+} ions on natural and chemically modified Nigerian kaolinite clay was investigated to determine the influence of chemical modification of the clay with 0.2 M solution of NaOH and ammonium oxalate. The adsorption of the metal ions as a function of pH, adsorbent particle size, adsorbent dose, agitation speed, initial metal ion concentration and temperature was investigated. Design-Expert software (version 10) was used to design the experiments based on response surface methodology for statistical optimization and to determine the extent of interaction of the parameters with contact time. Kinetic and adsorption isotherm models and thermodynamic parameters were used to evaluate the adsorption data. In addition, the clay adsorbents were characterized using microscopic and spectroscopic techniques.

MATERIALS AND METHODS
Preparation and Characterization of Clay Adsorbent
The clay sample (AK-clay) was obtained from a deposit in Argungu, Kebbi State, Nigeria. Separation of the clay particles from impurities was done by soaking it in deionized water for 24

hours and wet sieved with 63μm size sieve. Characterization of the clay was carried out using BRUKER, AXS D8 Advance X-Ray Diffractometer, Bruker Tensor 27 Platinum ATR-FTIR, TESCAN VEGA TS 5136LM Scanning Electron Microscope and Micrometrics Type Tristar II 3020 Surface Area Analyser.

Chemical Modification of Clay Adsorbent
The 63 μm fraction of AK-clay sample obtained after purification was modified using 0.2 M solution of sodium hydroxide (AK-S clay) and 0.2 M solution of ammonium oxalate (AK-AO clay). A 25 g portion of AK-clay was added to 500 mL of each solution and the suspension stirred with a magnetic stirrer at the rate of 200 revolutions per minutes (rpm) for 60 minutes at 50 ^{0}C. The resulting slurry was centrifuged at 3000 revolutions per minute (rpm) for 30 minutes and the sediment washed repeatedly with deionized water to neutral pH and dried at 103 ^{0}C.

Batch Adsorption
Stock solutions of Fe^{2+}, Pb^{2+}, Zn^{2+}, and Cr^{6+} were prepared by dissolving the calculated amount of analytical grade metal salts ($FeSO_4.7H_2O$, $Pb(NO_3)_2$, $ZnSO_4.7H_2O$ and $K_2Cr_2O_7$) in deionized water. A 0.25 L portion of aqueous solution (100 mg/L) of the heavy metal ion was contacted with the AK-clay in a thermostated shaker for 240 minutes during which 5.0 mL samples were withdrawn in the first 15 minutes and subsequently at time intervals of 30 minutes with the aid of a syringe. The samples withdrawn were centrifuged at 3500 revolutions per minute (rpm) for 15 minutes and the supernatant solution analyzed using Buck Scientific 210 VGP Atomic Absorption Spectrophotometer.

The effects of operational parameters including pH range of 2.0 - 5.5, 2.0 - 4.5, 2.0 - 7.0 and 2.0 - 10.0 for Fe^{2+}, Pb^{2+}, Zn^{2+} and Cr^{6+} ions, adsorbent particle size was in the range of 63 to 300 μm, adsorbent dosage in the range of 1.0 to 6.0 g/L, shaking speed (150 - 300 rpm), initial metal ion concentration (25 - 200 mg/L) and temperature (303 - 333 K) were investigated. At optimum conditions of the parameters, the effect of chemical modification was investigated by using AK-S and AK-AO clay for the adsorption of the

metal ions. Design-Expert Version 10 software (optimal custom design) was used to design the multi-factor experiments and to interpret the adsorption data obtained using RSM (Kalantari *et al.*, 2014; Biswas *et al.*, 2019).

The adsorption capacity of AK-clay was determined using the mass balance equation:

$$q_x = \frac{V(C_i - C_x)}{W} \tag{1}$$

where C_i and C_x are the initial and final concentrations of heavy metal ions (mg/L), V is the volume of metal ion solution used (L), W is the mass (g) of AK-clay and q_x is the amount of heavy metal ion adsorbed at equilibrium (mg/g).

The percentage of heavy metal ions removal was evaluated by using the formula:

Percentage removal (%) $= \frac{(C_i - C_x) \times 100}{C_i} \tag{2}$

The equilibrium adsorption data were analyzed using the following adsorption isotherm models:

Langmuir isotherm model: The linear form of the model equation is expressed as (Das *et al.*, 2014):

$$\frac{C_x}{q_x} = \frac{1}{bQ_0} + \frac{C_x}{Q_0} \tag{3}$$

where, C_x is the concentration of heavy metals in the solution at equilibrium (mg/L), q_x is the concentration of heavy metals in the solution at equilibrium (mg/g), b is Langmiur isotherm adsorption equilibrium constant (dm^3/mg) and Q_0 is the maximum monolayer coverage capacity (mg/g). The quantity C_x/q_x was plotted against C_x and the constants Q_0 and b calculated from the slope and the intercept respectively.

Freundlich isotherm model: The linear form of the equation is expressed as (Mahmoud, 2015):

$$\log q_x = \log K_f + \frac{1}{n} \log C_x \tag{4}$$

where, K_f is the Freundlich isotherm constant (mg/g) and n is the adsorption capacity. Log q_x was plotted against log C_x and the values of n and K_f determined from the slope and the intercept

respectively.

Tempkin isotherm model: Tempkin isotherm model equation in linear form is expressed as (Itodo and Itodo, 2010; Das *et al.*, 2014):

$$\frac{RT}{b_T} \ln A_T + \left(\frac{RT}{bT}\right) \ln C_x \tag{5}$$

where, A_T is Tempkin isotherm equilibrium binding constant (L/g), b_T is Tempkin isotherm constant related to the heat of adsorption (J/mol), T is temperature in Kelvin and R is the ideal gas constant (8.314 J/mol). The term q_x was plotted against $\ln C_x$ and the values of b_T and A_T obtained from the slope and the intercept respectively.

Dubinin-Radushkevich (D-R) isotherm model: D-R isotherm equation in linear form is expressed as (Subramanyam and Ashutosh, 2012):

$$\ln q_x = \ln q_A - \beta \varepsilon^2 \tag{6}$$

ε is Polanyi potential, which is equal to

$$\left[RT \ln \left(1 + \frac{1}{C_x} \right) \right] \tag{7}$$

where, q_A is the maximum adsorption capacity, R is the gas constant (8.314 $Jmol^{-1}$), T is the absolute temperature and β is the D-R isotherm constant (activity coefficient related mean adsorption energy E) (kj/mol). The term $\ln q_x$ was plotted against $[RT\ln(1 + \frac{1}{C_x})]^2$ and the values of β and q_A obtained from the slope and the intercept respectively.

The constant β which gives an idea about mean free energy E (kj/mol) of adsorption per molecule of the adsorbate using the relationship:

$$E = \frac{1}{\sqrt{2\beta}} \tag{8}$$

Flory-Huggins isotherm model: The model equation in linear form is expressed as (Theivarsu and Mylsamy, 2011):

$$\ln \left(\frac{\theta}{C_0} \right) = \log K_F + n \log(1 - \theta) \tag{9}$$

$$\theta = \left(1 - \frac{C_x}{C_0} \right) \tag{10}$$

where, θ is the degree of surface coverage, C_0 is the initial concentration of heavy metal ion (mg/L), n

is the number of adsorbate occupying adsorption sites and K_F is the equilibrium constant $(Lmol^{-1})$. K_F and n were determined from the plot of $\ln\left(\frac{\theta}{C_0}\right)$ versus $\log(1-\theta)$.

$$K_F = \exp\left(\frac{-\Delta G}{RT}\right) \tag{11}$$

Where, ΔA is the Gibbs free energy, R is gas constant $(8.314 Jmol^{-1}K^{-1})$ and T is absolute temperature in Kelvin.

The adsorption data were evaluated using the following kinetic models:

Pseudo first-order kinetic model: The linear form of the model rate equation used to evaluate the adsorption data is expressed as (Ho, 2004):

$$\log(q_x - q_t) = \log q_x - \left(\frac{k_1}{2.303}\right)t \tag{12}$$

where, q_x is the amount of metal ion in the adsorbent at equilibrium (mg/g), q_t is the amount of metal ion adsorbed at time (t) and k_1 is the rate constant of the pseudo first order equation (min^{-1}). The term $\log(q_x - q_t)$ was plotted against t and the constants k_1 and q_x calculated from the slope and the intercept respectively.

Pseudo second-order kinetic model: Equation for the kinetic model is expressed as (Das *et al.*, 2014):

$$\frac{t}{q_t} = \frac{1}{k_2 q_{2x}} + \frac{1}{q_x}t \tag{13}$$

where, k_2 is the rate constant of the pseudo second order equation $(gmg^{-1}min^{-1})$. The term $\frac{t}{q_t}$ was plotted against t and the constants q_x and k_2 obtained from the slope and the intercept respectively.

Elovich kinetic model: The simplified linearized Elovich kinetic model is expressed as (Ho, 2004):

$$q_t = \frac{1}{\beta}\ln(\alpha\beta) + \frac{1}{\beta}\ln t \tag{14}$$

where, β is the desorption constant. The term q_t was plotted against $\ln t$ and values of β and α obtained from the slope and the intercept respectively.

Intra-particle diffusion model: The equation is expressed as (Das *et al.*, 2014):

$$q_t = Kt^{1/2} + C \tag{15}$$

where, *k* is the rate constant at equilibrium and *C* is the film thickness. The term qt was plotted against $t^{1/2}$ and the values of K and *C* obtained from the slope and the intercept respectively.

Thermodynamic parameters which include Gibbs free energy change (ΔG°), enthalpy change (ΔH°) and entropy change (ΔS°) were determined using the following equations:
ΔH° and ΔS° is calculated using Vant't Hoff equation (Nethaji *et al.*, 2013):

$$\ln K_{eq} = \frac{\Delta S^0}{R} - \frac{\Delta H^0}{RT} \tag{16}$$

The values of ΔH° and ΔS° were obtained from the slope and intercept of the plot of $\ln K$ versus $\frac{1}{T}$, where K_{eq} is the equilibrium constant.

The value of ΔG° was calculated using the expression (Anastopoulos and Kyzas, 2016):
$$\Delta G^\circ = -RT\ln K_{eq} \tag{17}$$
where, R is the gas constant, T is temperature in Kelvin. Constant K_{eq} was made dimensionless by multiplying it value with the molecular weight of the metal ion and concentration of metal ion solution in selected standard rate (Mole water per liter i.e. 1000 g divided by molar mass of water) (Liu, 2009; Zhou and Zhou, 2014).

RESULTS AND DISCUSSION
Characterization of Natural Kaolin (AK-clay) and Chemically Modified Kaolinite Clay (AK-AO and AK-S)
XRD: The diffraction peaks for the interlayer spacing of AK-clay were predominantly observed at 12.4, 25, 38.5, 55 and 62.5^0 2θ (Figure 1). This pattern confirms kaolinite as the only clay mineral present in the 63 µm fraction of the clay. Similar diffraction peaks for kaolinite clay have been reported in literature (Olokode *et al.*, 2010; Zhu *et al.*, 2016).

BET: The surface area and pore structure parameter results of AK-clay are presented in Table 1. The single point surface and BET surface area were 21.349 and 6.295 m^2/g respectively. The

Langmuir surface area and t-plot which defined the statistical thickness of adsorbed multilayer on the pore surface area were 65.204 and 25.545 m^2/g respectively. This result is similar to a recent report of surface area characterization of kaolinite clay (Panda _et al._, 2013). Variation in surface area and pore parameters were observed after modification of AK-clay with NaOH (AK-S) and ammonium oxalate (AK-AO) clay. AK-AO clay recorded an increase in single point surface area from 21.335 to 22.001 m^2/g while surface area measured by BET method increased from 6.295 to 7.364 m^2/g. Langmuir surface area and pore volume equally showed significant increase while t-plot external surface area and desorption average pore diameter diminished. The increase in surface area can be attributed to the smaller size effect of the oxalate ion which increased the accessibility of nitrogen gas into the internal surface of the clay (Xi _et al._, 2010; Qiao _et al._, 2015). Single point, BET and Langmuir surface area measurement and other pore structure parameters of AK-S clay showed significant decrease in values. As observed in this study, variation in structural parameters of clays as a result of modification has been reported (Kooli _et al._, 2006; Xi _et al._, 2010).

FTIR: The two strong absorption bands observed at 3689 and 3619 cm^{-1} represent stretching of the surface hydroxyl groups of the dioctahedral layer and inner hydroxyl groups located in the plane between the tetrahedral and octahedral sheets (Figure 2a). These peaks confirmed that the clay is kaolin and is in agreement with literature report (Osabor _et al.,_

2009; Djomgoue and Njopwouo, 2013). Absorption peaks at 1634, 1114, 1025, 998 and 909 cm^{-1} correspond to deformation band of water, Si-O-Si stretching, in-plane Si-O stretching, Si-OH stretching and deformation bands of Al-Al-OH respectively. Two intensive peaks at 749 and 788 cm^{-1} were assigned to Al-O and Si-O out of plane respectively. These assignments are similar to those reported (Vaculikora and Plevora, 2005). After modification of AK-clay with 0.2M solution of NaOH and 0.2M solution of ammonium oxalate, no major significant shift was recorded for the hydroxyl groups stretching, A-Al-OH bending and Si-O bending. However, sharp intense peak, broad medium band and sharp band observed at 1634, 1375 and 1250 cm^{-1} (Figure 2c) were assigned to C=O, C-O stretching and O=C-O symmetric of the oxalate in AK-AO clay (Fan _et al._, 2010).

SEM: Analysis of SEM microstructure of the natural and chemically modified clays are shown in Figure 3 (a-c). The orientation of AK-clay exhibits a predominant filmy particles stack in layers. The micrographs of AK-S clay show variable cluster of flake-like particles, while AK-AO clay is composed of largely filmy flaked particles that are loosely packed with some level of porosity which improves the adsorption capacity of the clay. Closely packed layers of particles and flaky dispersed fractions with more micro-sized particles of larger surface area after modification of a kaolinite clay has been reported (Jiang _et al._, 2009).
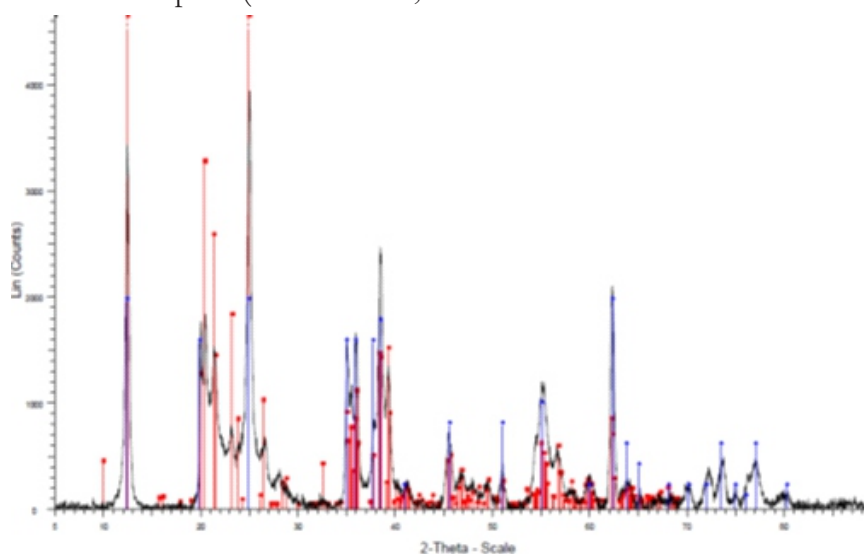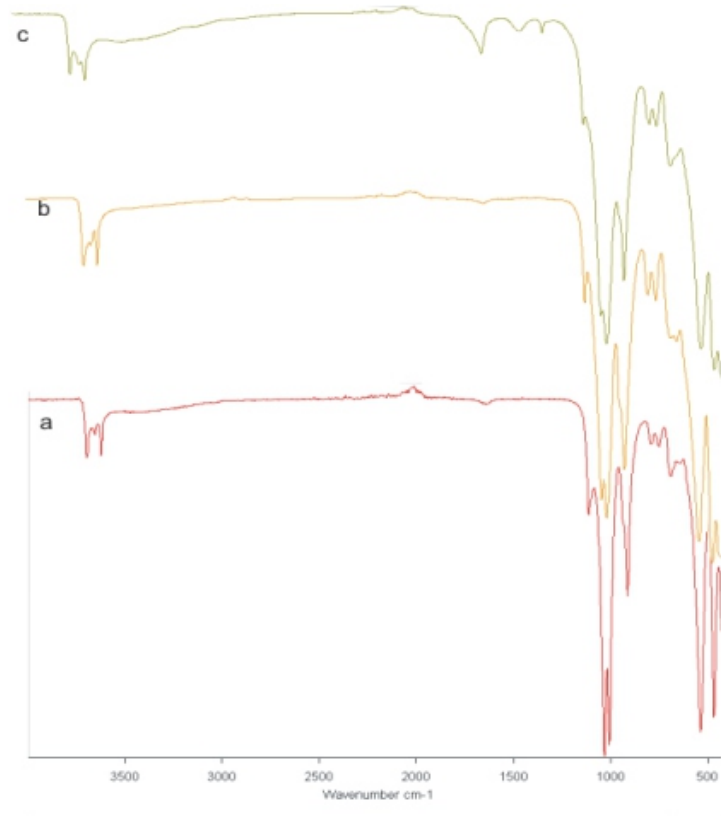

Figure 1: XRD pattern of AK-clay

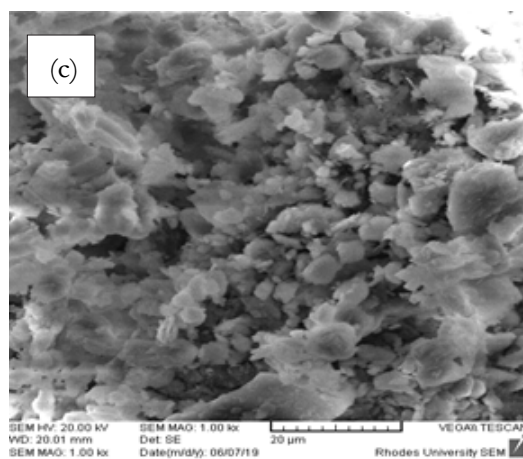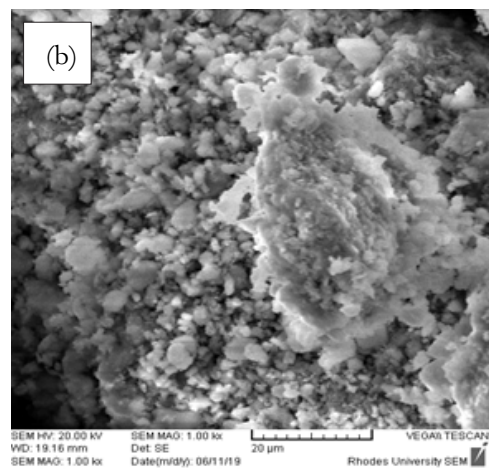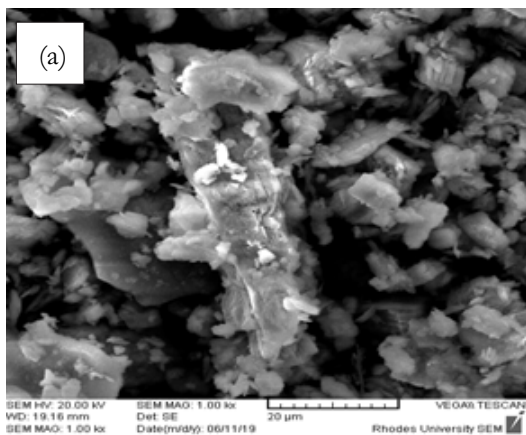Figure 2: FTIR spectra for: (a) AK-clay (b) AK-S (c) AK-AO

Figure 3: SEM photography of: (a) AK-clay (b) AK-S (c) AK-AO clay

Table 1. Surface area pore parameters of AK-clay, AK-S clay and AK-AO clay

Adsorbent	AK-clay	AK-S clay	AK-AO clay
Surface area (m^2/g)			
Single point surface area at P/P$_o$	21.3349	14.0029	22.0001
BET surface area	6.2946	4.2503	7.3641
Langmuir surface area	65.2504	55.113	67.7028
t-Plot external surface area	25.5449	17.2229	24.1422
BJH Adsorption cumulative surface area of pores between 17.000 Å to 3,000.000 Å	26.131	21.475	28.281
BJH Desorption cumulative surface area of pores between 17.000 Å to 3,000.000 Å	30.3336	23.5978	30.6004
Pore Volume (cm^3/g)			
Single point adsorption total pore volume of pores < 111.415 Å diameter at P/P$_O$	-	0.003169	-
BJH Adsorption cumulative volume of pores between 17.000 Å to 3,000.000 Å	0.038368	0.031001	0.040975
BJH Desorption cumulative volume of pores between 17.000 Å to 3,000.000 Å	0.043250	0.033193	0.041669
Pore Size (Å)			
Adsorption average pore diameter (4V/A by BET)	-	29.8214	-
BJH Adsorption average pore width (4V/A)	58.731	58.744	57.954
BJH Desorption average pore width (4V/A)	57.033	56.264	54.469

Adsorption Results for Fe^{2+}, Pb^{2+}, Zn^{2+} and Cr^{6+} Ions on AK-Clay

Effect of pH

The results of effect of pH on adsorption of Fe^{2+}, Pb^{2+}, Zn^{2+} and Cr^{6+} ions on AK-clay are presented in Figure 4 (a-b). The adsorption experiment were performed in pH range as stated in batch adsorption section because precipitation of the metals occurred at pH above 5.5, 4.5 and 8.0 for Fe^{2+}, Pb^{2+} and Zn^{2+} ion respectively. Precipitation of metal hydroxides have been established to occur above certain pH (Donat _et al._, 2005; Cheng _et al._, 2012), The adsorption of Fe^{2+} ion increased significantly as the pH increased from 2.0 to 5.0 with optimum removal efficiency of 26.2 % (6.55 mg/g). As the pH was increased from 5.0 to 5.5, the rate of adsorption decreased due to hydrolysis of Fe^{2+} ion at higher pH (Cheng _et al._, 2012). Adsorption of Pb^{2+} ion increased as the pH increased from 2.0 to 4.5 to an optimum removal

efficiency of 56.9 % (14.23 mg/g). The retention capacity of Zn^{2+} ion increased as the pH increased from 2.0 to 6.0 at optimum uptake of 35 % (8.75 mg/g). A decline in uptake recorded at pH of 7 can be attributed to a decrease in electrostatic attraction as a result of transition of zinc from ionic state to $Zn(OH)_2$ (Chai _et al._, 2017). Optimum uptake of 23.3 % (5.825 mg/g) was recorded at pH of 4.0 for Cr^{6+} ion. The decrease in adsorption trend on both sides of this pH value was attributed to hydrogen ion competing for adsorption at lower pH and formation of hydroxide complexes of chromium which hinders the diffusion on the kaolinite clay surface at higher pH value. Substantial uptake of Cr^{6+} at pH < 4 was attributed to the binding of Cr^{6+} ion to hydroxyl group in the anionic form (hydrochromate) of $HCrO_4$- (Griffin _et al._, 1977; Bhattacharyya and Gupta, 2008).
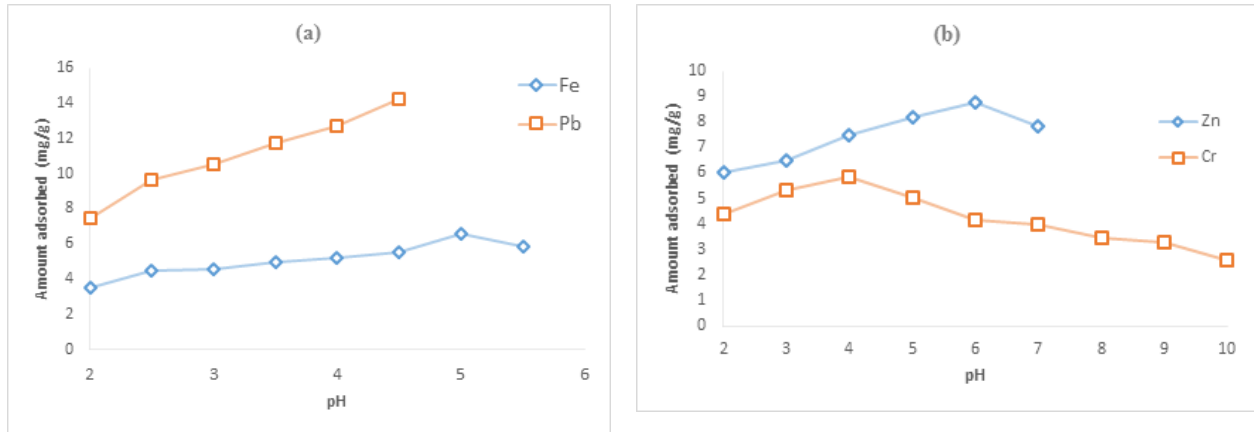
Figure 4: Effect of pH on adsorption of: (a) Fe^{2+} and Pb^{2+} ions (b) Zn^{2+} and Cr^{6+} ions.
Conditions: Particle size, 63 μm; adsorbent dose, 4.0 g/L; temperature, 313K; shaking speed, 250 rpm; initial metal ion concentration, 100 mg/L.

Effect of Particle Size

The results of effect of particle size on the adsorption of the metal ions on AK-clay are presented in Figure 5. The optimum uptake of the metal ions was recorded with particle size 63 μm as 35 % (8.75 mg/g) for Zn^{2+} ion and 39.3 % (9.825 mg/g), 60 % (15.0 mg/g) and 23.3 % (5.825 mg/g) with particle size 75 μm for Fe^{2+}, Pb^{2+} and Cr^{6+} ions respectively. As the particle size increased (75 - 300 μm), the amount of metal ions adsorbed decreased significantly from 9.825 to 3.675 mg/g, 15.0 to 11.075 mg/g, 8.75 to 5.75 mg/g and 5.825 to 3.775 mg/g for Fe^{2+}, Pb^{2+}, Zn^{2+} and Cr^{6+} ions respectively. This is in agreement with literature data which indicate that smaller particle size exposes more active sites for adsorption as a result of increased surface area for effective contact with adsorbed solute molecules (Arivoli *et al.*, 2013; Dawodu and Akpomie, 2014).

The three-dimensional (3D) response surface graphs show that particle sizes 63 and 75 μm favour the adsorption of Fe^{2+}, Pb^{2+} and Cr^{6+} ions while only particle size 63 μm favours Zn^{2+} ion. From Analysis of Variance (ANOVA) and model statistics results, quartic equation was found to best describe the effect of particle size for the metal ions with p-value < 0.0001 at 95 % confidence limit and F-values of 1038.12, 343.85, 304.55 and 150.79 for Fe^{2+}, Pb^{2+}, Zn^{2+} and Cr^{6+} ions respectively.
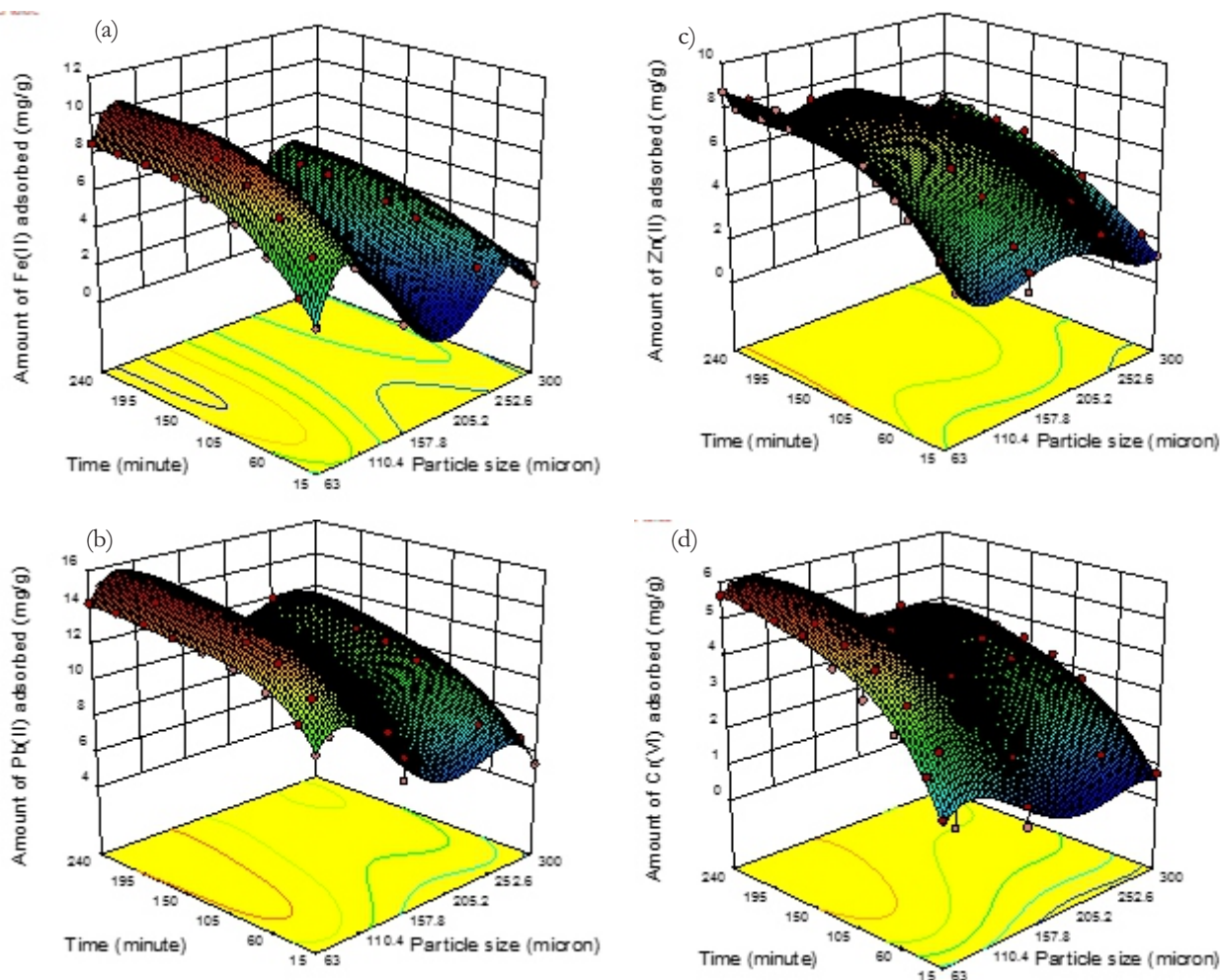
Figure 5: 3D plots for effect of particle size: (a) Fe^{2+} (b) Pb^{2+} (c) Zn^{2+} (d) Cr^{6+}.
Conditions: pH, value 5.0, 4.5, 6.0 and 4.0 for Fe^{2+}, Pb^{2+}, Zn^{2+} and Cr^{6+} ion; adsorbent dose, 4.0 g/L; temperature, 313 K; shaking speed, 250 rpm; initial metal ion concentration, 100 mg/L.

Effect of Adsorbent Dose

The sequence of uptake for the metal ions in 3D response surface plot is presented in Figure 6. As the concentration of adsorbent increased from 1.0 to 4.0 g/L, the amount of Fe^{2+}, Zn^{2+} and Cr^{6+} ions adsorbed increased from 14 to 39.3 %, 12.1 to 65 % and 11.1 to 23.3 % while the metal ion adsorbed per unit mass decreased from 14.0 to 9.83 mg/g, 12.1 to 8.75 mg/g, and 11.1 to 5.83 mg/g for Fe^{2+}, Zn^{2+} and Cr^{6+} ions respectively. The decrease in mass of adsorbed metal ion per unit mass of adsorbent as the adsorbent weight increase was attributed to decrease in adsorbate-adsorbent ratio as adsorbent weight increased (Sari *et al.*, 2007). Further increase in AK-clay weight from 4.0 to 6.0 g/L was characterized by low increase in percentage adsorption of the three metal ions. This was attributed to aggregation of adsorbent particles which decreased the available

external surface area and overlapping of adsorption sites (Bernard *et al.*, 2013). Thus, 4.0 g/L was found to be the most suitable adsorbent concentration for Fe^{2+}, Zn^{2+} and Cr^{6+} ions. In the case of Pb^{2+} ion, the adsorption capacity increased steadily as the weight of AK-clay increased from 1.0 g/L (35.0 %, 35.0 mg/g) to 5.0 g/L (72 %, 14.925 mg/g). No further significant increase was observed as the weight of AK-clay was increased to 6.0 g/L.

As shown in the 3D graphs, the near state of adsorption equilibrium for the metal ions was attained for low adsorbent concentration of 1.0 g/L at contact time of 180 minutes for Cr^{6+} ion and 150 minutes for Fe^{2+}, Pb^{2+} and Zn^{2+} ion respectively. However, as the adsorbent concentration increased, the equilibrium contact time decreased significantly to 60 minutes at 6.0

g/L of adsorbent weight for all the metal ions. Similar findings of decrease in adsorption capacity of kaolinite clay as the adsorbent dosage increased has been reported in literature (Ajemba, 2014; Das *et al*., 2014). The relationship between adsorbent dose and contact time was described by Fifth polynomial model. The p-values < 0.0001 at 95 % confidence limit and F-values of 376.27, 740.38, 249.73 and 312.68 for Fe^{2+}, Pb^{2+}, Zn^{2+} and Cr^{6+} ions observed, showed the model is statistically significant.
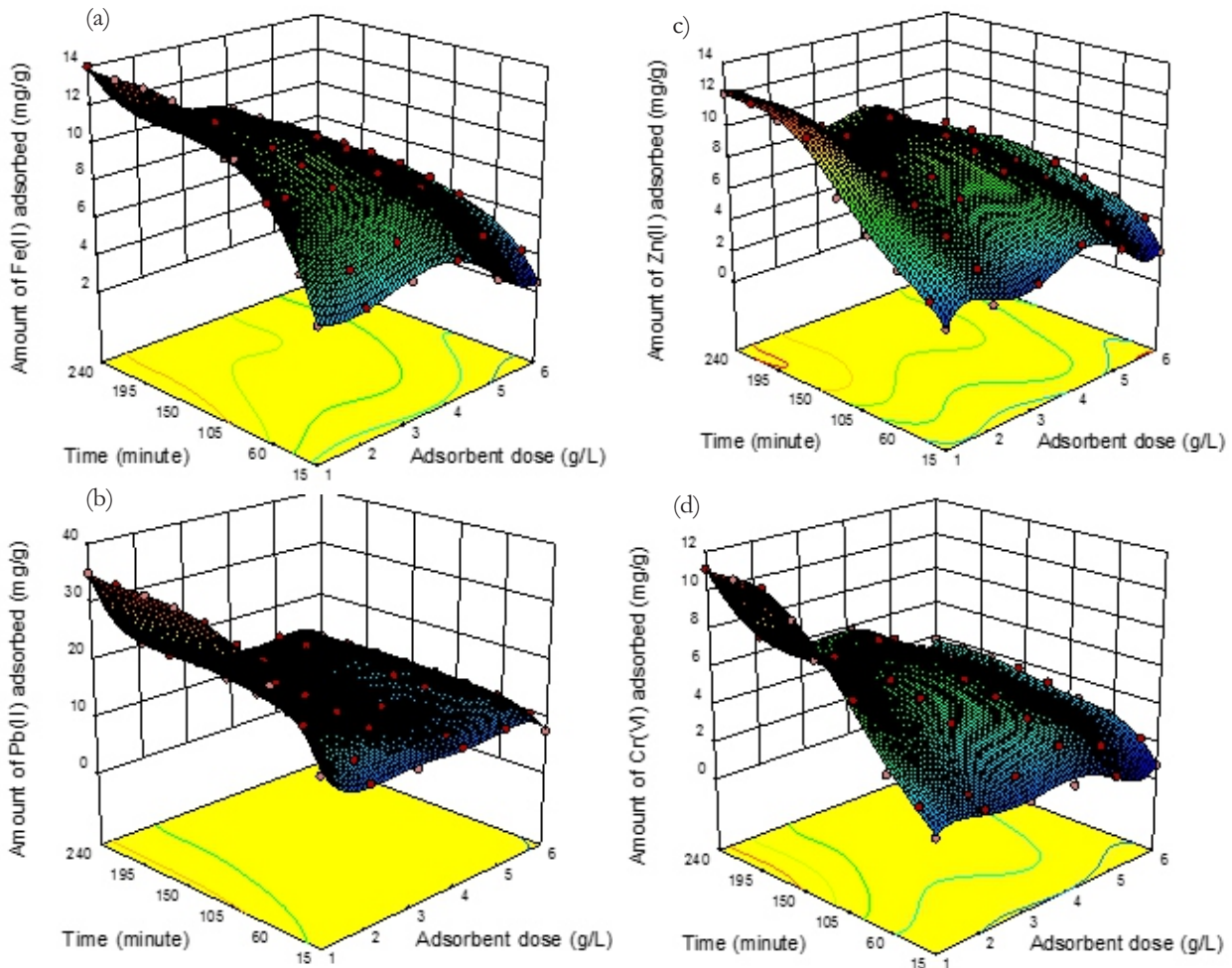

Figure 6: 3D plots for effect of adsorbent dose: (a) Fe^{2+} (b) Pb^{2+} (c) Zn^{2+} (d) Cr^{6+}.
Conditions: pH, 5.0, 4.5, 6.0 and 4.0 Fe^{2+}, Pb^{2+}, Zn^{2+} and Cr^{6+}; particle size, 63 μm for Zn^{2+} and 75 μm for Fe^{2+}, Pb^{2+} and Cr^{6+}; temperature, 313 K; shaking speed, 250 rpm; initial metal ion concentration, 100 mg/L.

Effect of Shaking Speed

The effect of shaking speed on adsorption of the metal ions is presented in Figure 7. The optimum adsorption capacity of 5.825 mg/g (23.3 %) for Cr^{6+} ion was obtained at agitation speed of 250 rpm while at 300 rpm, adsorption capacity of 11.875 mg/g (47.5 %), 16.0 mg/g (80.0 %) and 9.975 mg/g (39.9 %) were achieved for Fe^{2+}, Pb^{2+} and Zn^{2+} ions respectively. Increase in agitation speed generally increased the rate of diffusion of ions to the adsorbent and reduce film boundary layer around the adsorbent (Bingol *et al*., 2005;

Bernard *et al*., 2013). However, the decline in uptake of Cr^{6+} ion as the agitation speed increased from 250 rpm (23.3 %, 5.825 mg/g) to 300 rpm (22.0 %, 5.5 mg/g) may be due to possible breakage of bond between the Cr^{6+} ion and active site as a result of additional energy (Doss and Kodolikar, 2012).

The 3D sloppy pattern of graphs observed for Fe^{2+}, Pb^{2+} and Zn^{2+} ions, shows the rate of their adsorption increased rapidly as the agitation speed increased from 150 to 300 rpm. Uptake of Cr^{6+} ion

presented a peak that shows its adsorption recorded no significant increase in agitation speed between 200 to 300 rpm. The Cubic model equation model was found to fit the ANOVA analysis for Fe^{2+}, Pb^{2+} and Zn^{2+} ions, while quadratic polynomial model best suited the

analysis of Cr^{6+} ion adsorption process. The statistical P-value < 0.0001 at 95 % confidence limit and F-values of 1287.75, 681.85, 471.89 and 32.43 obtained for Fe^{2+}, Pb^{2+}, Zn^{2+} and Cr^{6+} ions respectively, implies the models are significant for shaking speed and contact time interaction.
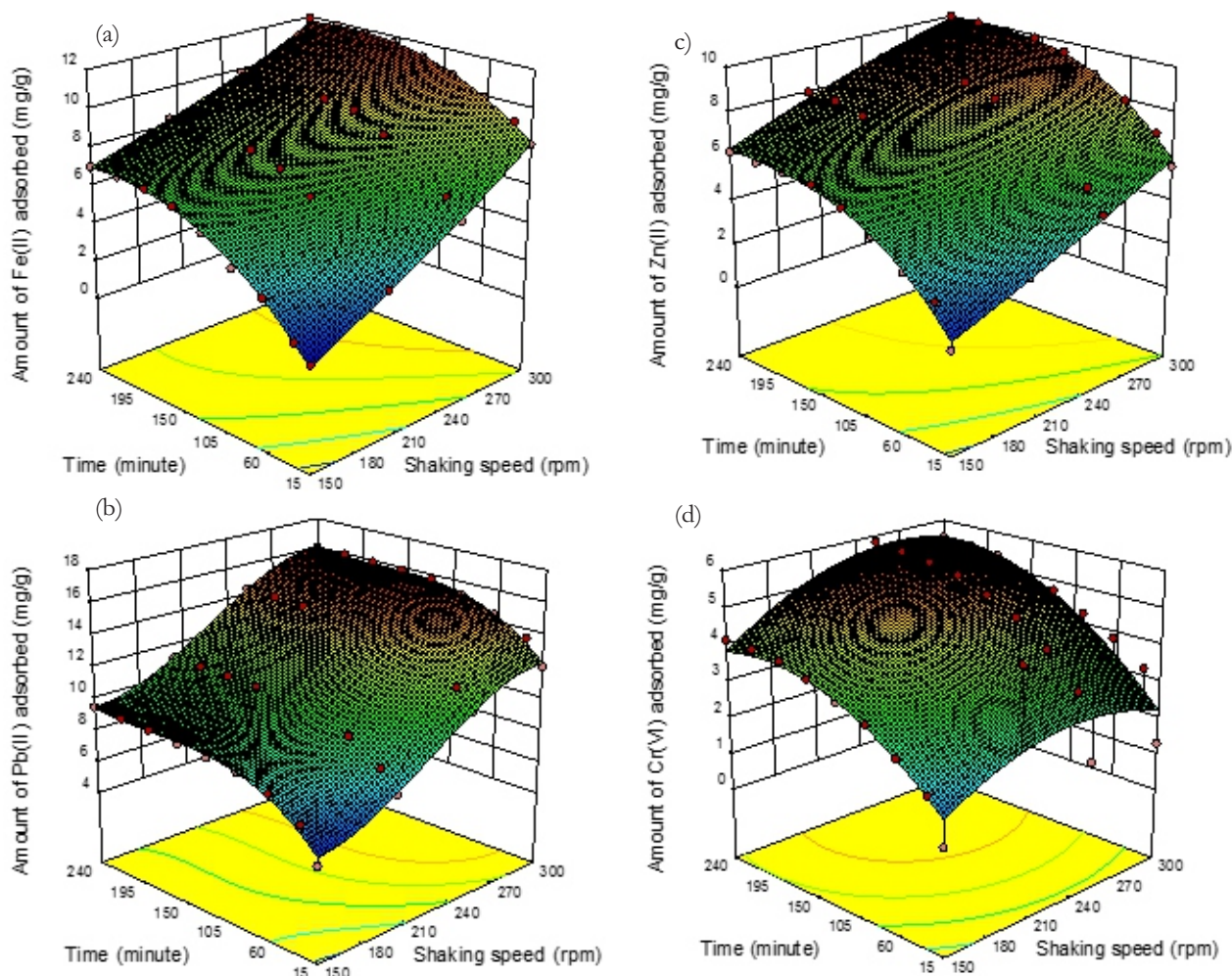

Figure 7: 3D response surface for effect of shaking speed: (a) Fe^{2+} (b) Pb^{2+} (c) Zn^{2+} (d) Cr^{6+}. Conditions: pH, 5.0, 4.5, 6.0, and 4.0 for Fe^{2+}, Pb^{2+}, Zn^{2+} and Cr^{6+}; particle size, 63 μm for Zn^{2+} and 75 μm for Fe^{2+}, Pb^{2+} and Cr^{6+}; adsorbent dose, 4.0 g/L for Fe^{2+}, Zn^{2+} and Cr^{6+} and 5.0 g/L for Pb^{2+}; temperature, 313 K; initial metal ion concentration, 100 mg/L.

Effect of Initial Metal Ion Concentration The effect of initial metal ion concentration on the adsorption capacity of AK-clay for all the metal ions is presented in Figure 8. The percentage adsorption of Fe^{2+} ion was high with removal rate of 90.4 % (5.65 mg/g) and 92.0 % (11.5 mg/g) at initial concentrations of 25 and 50 mg/L respectively. As the initial metal ion concentration increased, the percentage uptake reduced while the adsorption capacity increased to 47.5 %

(11.875 mg/g), 32 % (12.25 mg/g) and 27.7 % (13.85 mg/g) at 100, 150 and 200 mg/L respectively. The decrease in percentage removal as the initial concentration increased from 25 to 200 mg/L can be attributed to more metal ions competing for fixed binding sites available for interaction. However, the increase in adsorption capacity of the adsorbent as the initial concentration increased is facilitated by increase in driving force of the metal ion towards the active

sites (Jiang *et al.*, 2009; Aliabadi *et al.*, 2012). At initial Pb^{2+} ion concentrations of 25, 50, 100, 150 and 200 mg/L, the amount of Pb^{2+} ion adsorbed were 4.54 mg/g (90.8 %), 9.04 mg/g (90.4 %), 16.0 mg/g (80 %), 23.4 mg/g (78.0 %) and 30.8 mg/g (77.0 %) respectively. High adsorption percentage of 93.2 % (5.83 mg/g) and 78 % (9.75 mg/g) at initial concentrations of 25 and 50 mg/L were recorded for Zn^{2+} ion. As the initial concentration increased, the percentage adsorption declined while the adsorption capacity increased as 39.9 % (9.975 mg/g), 43.33 % (16.25 mg/g) and 35.0 % (17.5 mg/g) for initial concentrations of 100, 150 and 200 mg/L respectively. The rate of adsorption of Cr^{6+} ion adsorbed at initial concentrations of 25 and 50 mg/L were 5.05 mg/g (80.8 %) and 5.75 mg/g (46.0 %) respectively. Further increase in initial concentration resulted in increase in adsorption capacity while the percentage adsorption diminished as follows: 5.825 mg/g (23.3 %), 8.675 mg/g (23.13 %) and 9.0 mg/g (18.0 %) for initial concentrations of 100, 150 and 200 mg/L respectively.

The 3D graphs revealed the interactive effect of initial concentration with contact time. The patterns showed a major increase in adsorption as initial concentration of Fe^{2+} ion increased from 25 to 50 mg/L with near state of equilibrium at contact time of 60 minutes. From 50 to 150 mg/L, no major significant increase in rate of uptake occurred as observed in the response surface pattern. However, a rise in adsorption of Fe^{2+} ion and a reduction in equilibrium contact time of 20 minutes was observed when the initial

concentration increased to 200 mg/L. For Pb^{2+} and Zn^{2+} ions, the 3D graph pattern revealed major increase in their adsorption as the initial concentrations increased from 25 to 200 mg/L. For Cr^{6+} ion, no major significant increase was observed as initial concentration increased from 25 to 100 mg/L. But rapid increase at concentrations of 150 to 200 mg/L was obtained. From the results, it was observed that adsorption of the metal ions recorded over 90% removal at low initial metal ion concentrations of 25 and 50 mg/L. However, as the initial metal ion concentrations increased, the adsorption capacities of the adsorbents increased due to the number of molecules of solute available for interaction per unit mass of adsorbent. But the overall percentage showed a decreasing trend as a result of overcrowding of adsorbed molecules around the fewer available active sites (Bhattacharyya and Gupta, 2011; Das *et al.*, 2014). The decrease in percentage removal of the metal ions from aqueous solutions and increase in adsorption capacity as reported in this study is in agreement with literature (Aliabadi *et al.*, 2012; Rane and Japkal, 2014). From ANOVA and model Statistics obtained from the response surface, polynomial in quartic equation model fits adsorption data. The p-values < 0.0001 at 95 % confidence limit and relatively high F-values of 462.82, 757.80, 136.07 and 153.94 obtained for Fe^{2+}, Pb^{2+}, Zn^{2+} and Cr^{6+} ion respectively, showed the model is significant for the range of initial metal ion concentrations and contact times studied.
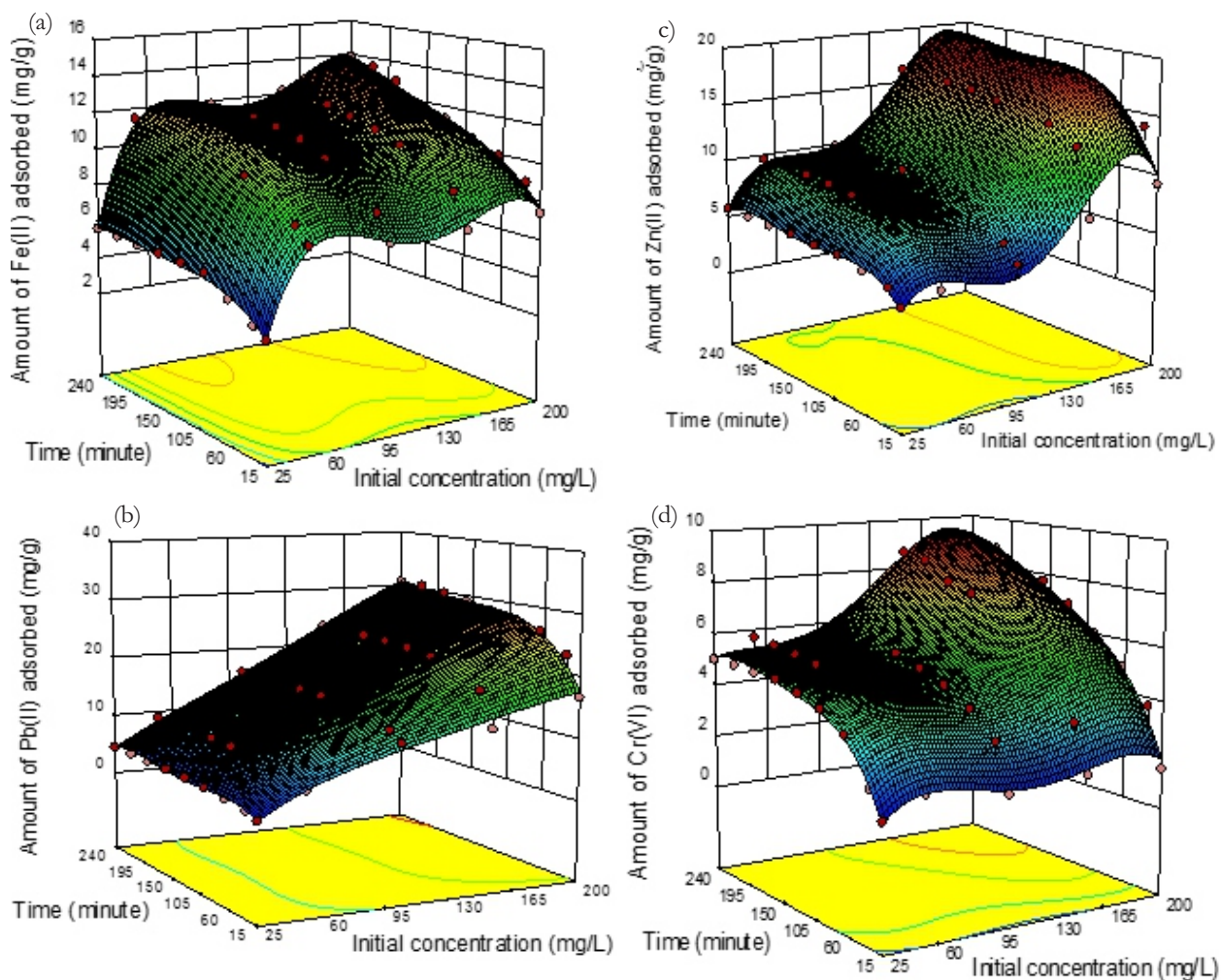
Figure 8: 3D response surface for effect of initial concentration: (a) Fe^{2+} (b) Pb^{2+} (c) Zn^{2+} (d) Cr^{6+}. Conditions: pH, 5.0, 4.5, 6.0, and 4.0 for Fe^{2+}, Pb^{2+}, Zn^{2+} and Cr^{6+}; particle size; 63 µm for Zn^{2+} and 75 µm for Fe^{2+}, Pb^{2+} and Cr^{6+}; adsorbent dose, 4.0 g/L for Fe^{2+}, Zn^{2+} and Cr^{6+} and 5.0 g/L for Pb^{2+}; temperature, 313 K.

Effect of Temperature

The results presented in Figure 9 showed the adsorption of Fe^{2+} and Zn^{2+} ions increased as the temperature increased from 303 to 333 K with optimum capacity of 14.10 mg/g (56.4 %) and 17.94 mg/g (89.7 %) respectively. Increase in temperature has been reported to increase the force of attraction which causes the ions to migrate from bulk liquid phase to the outer surface by film diffusion and subsequently into the micro and macro-pores of the clay (pore diffusion) for interaction at the active sites (Adebowale *et al.*, 2008; Khansaa and Fawwaz, 2018). The optimum adsorption recorded for Pb^{2+} ion was 18.4 mg/g (92.0 %) at 328 K and 7.65 mg/g (30.6 %) at 323 K for Cr^{6+} ion respectively. Above these temperatures, a decrease in the uptake was observed for both Pb^{2+} and Cr^{6+} ions. This can be

attributed to desorption tendency from the solid liquid interface to the solution at relatively high temperature (Sari *et al.*, 2007).

The 3D pattern for Fe^{2+} ion shows its adsorption increased rapidly with increase in temperature from 303 to 313 K. A minimal increase in removal efficiency was observed as the temperature increased further from 313 to 333 K. For Pb^{2+}, Zn^{2+} and Cr^{6+} ions, the slopes of the graph increased rapidly which indicate increase in uptake of the ions as temperature increased from 303 to 328 K for Pb^{2+}, 303 to 333 K for Zn^{2+} and 303 to 318 K for Cr^{6+} ion respectively. Above these optimum temperatures, a decline in increase in adsorption was observed for removal efficiency for Pb^{2+}, Zn^{2+} and Cr^{6+} ions. From the ANOVA

and Model Statistics analysis, polynomial in sixth degree model fits the adsorption of Fe^{2+} and Pb^{2+} ions, fifth degree model for Zn^{2+} ion and quadratic model for Cr^{6+} ion respectively. The p-values < 0.0001 at 95 % confidence limit and F-values of 637.02, 1054.75, 647.15 and 54.03 obtained for Fe^{2+}, Pb^{2+}, Zn^{2+} and Cr^{6+} ions respectively, implies the models are significant for the combined factors of temperature and contact time.
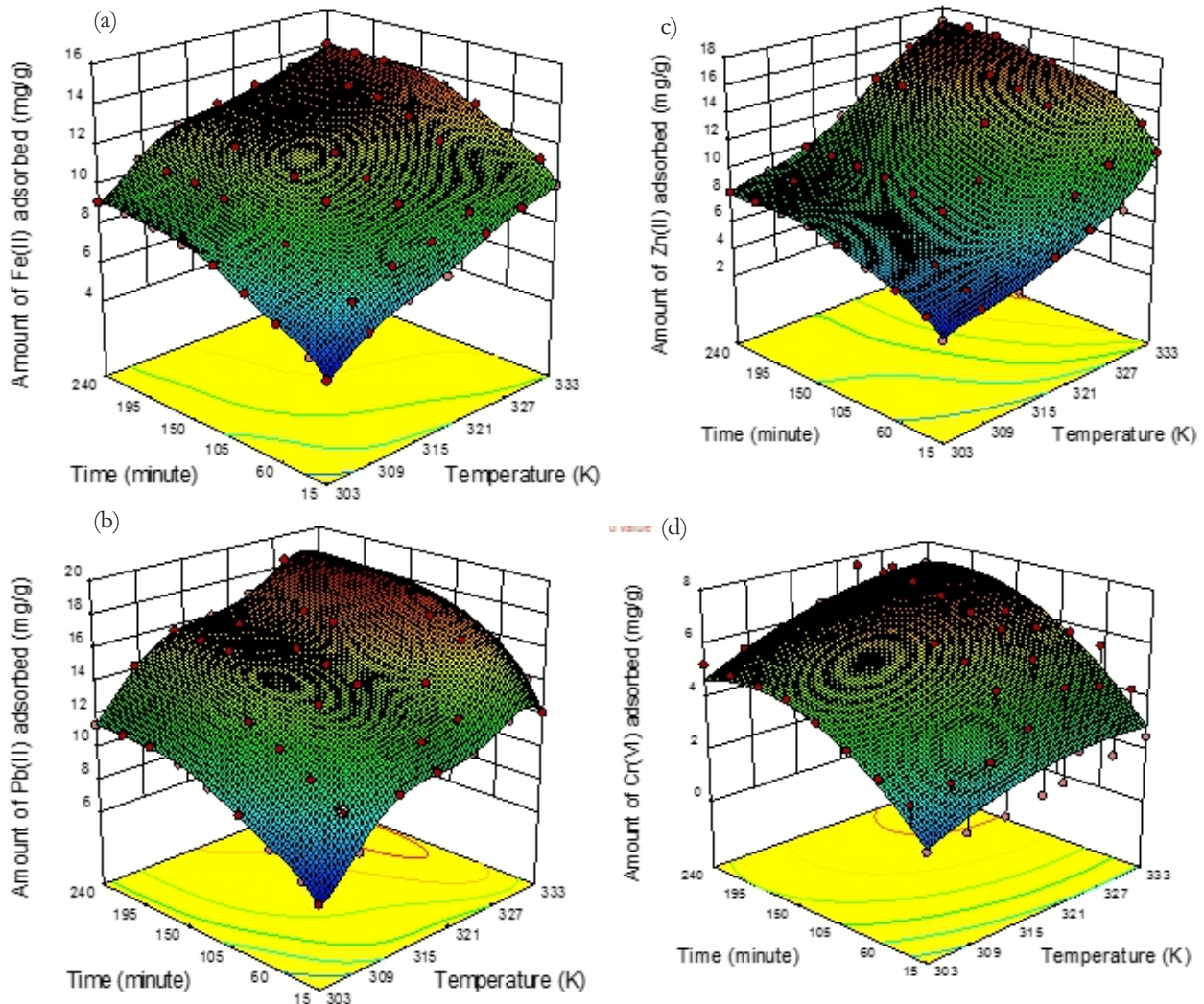

Figure 9: 3D response surface for effect of temperature: (a) Fe^{2+} (b) Pb^{2+} (c) Zn^{2+} (d) Cr^{6+}. Conditions: pH, 5.0, 4.5, 6.0 and 4.0 for Fe^{2+}, Pb^{2+}, Zn^{2+} and Cr^{6+} ions; particle size, 63μm for Zn^{2+} and 75 μm for Fe^{2+}, Pb^{2+} and Cr^{6+}; adsorbent dose, 4.0 g/L for Fe^{2+}, Zn^{2+} and Cr^{6+} and 5.0 g/L for Pb^{2+}; agitation speed, 250 rpm for Cr^{6+} and 300rpm for Fe^{2+}, Pb^{2+}, Zn^{2+}; initial metal ion concentration, 100 mg/L.

Adsorption of Metal Ions on Chemically Modified (AK-S and AK-AO) Clays
As shown in Figure 10, there was increase in the adsorption capacity of the natural clay after modification with NaOH (AK-S) and ammonium oxalate (AK-AO).The adsorption of Fe^{2+} ion increased from 14.1 mg/g (56.4 %) to 17.375 mg/g (69.5 %) and 18.425 mg/g (73.7 %) for AK-AO and AK-S clay respectively. Also, the adsorption of Zn^{2+} ion increased from 16.875 mg/g (67.5 %) to 16.95 mg/g (67.8 %) and 19.9

mg/g (79.6 %) for AK-AO and AK-S clay respectively. Only AK-S clay showed increase in the adsorption of Pb^{2+} ion from 18.4 to 19.8 mg/g (92 to 99.0 %) while little increase from 7.65 to 8.15 mg/g (30.6 to 32.6 %) was observed for Cr^{6+} ion. From the results, modification of AK-clay with ammonium oxalate increased its adsorption capacity for only Fe^{2+} and Zn^{2+} ions while NaOH modified clay increased the adsorption capacity for all the metal ions. The increase in adsorption efficiency recorded with AK-S clay was due to

increase in porosity and saturation of negatively charged hydroxyl anions that enhanced adsorption of positively charged metal ions through electrostatic force of attraction (Jiang *et al.*, 2010; Meroufel *et al.*, 2013). The ability of AK-AO clay to increase in the adsorption of Fe^{2+} and Zn^{2+} ions can be attributed to the increase the porosity of AK-AO clay and ease of NH_4^+ ion replacement by the incoming metal ions. This is

supported by the increase in surface area and other pore structure parameters recorded after modification AK-clay with ammonium oxalate (Table 1). Furthermore, the oxalate ion bonded at the surface of the clay possess the ability to selectively form complexes with some metal ions with high binding capacity (Mielniczek-Brzohska *et al.*, 2000; Lee *et al.*, 2000; Stoppe *et al.*, 2015).
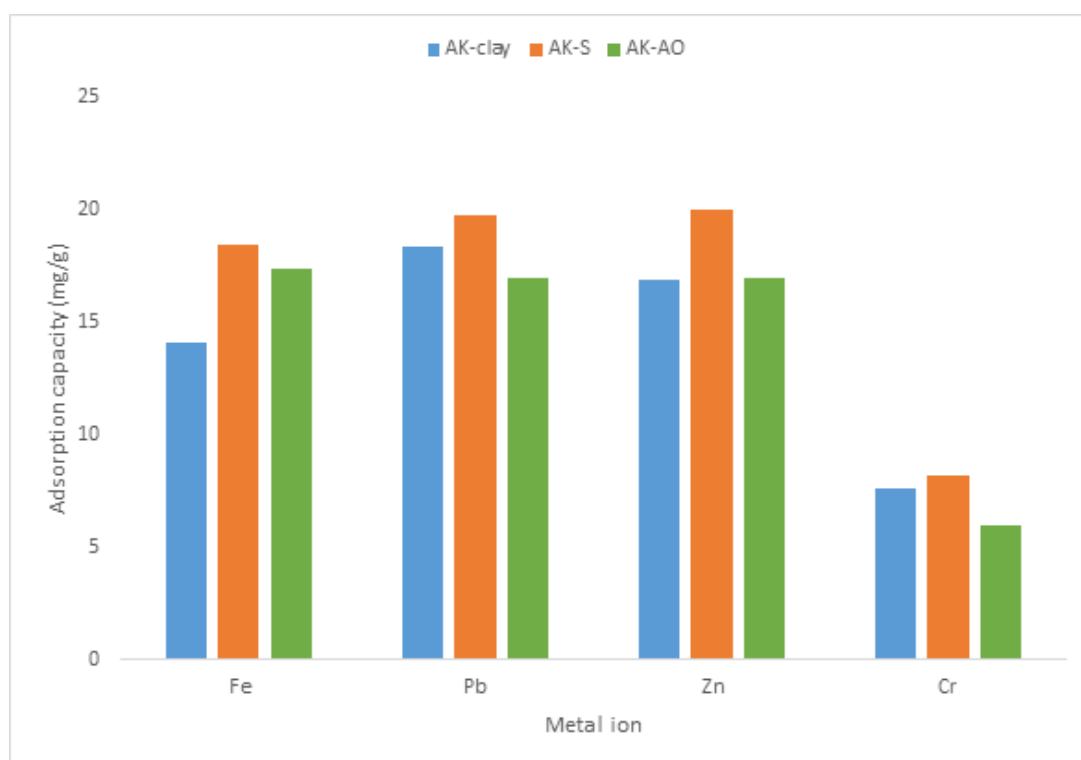

Figure 10: Effect of chemical modification.
Conditions: pH, 5.0, 4.5, 6.0 and 4.0 for Fe^{2+}, Pb^{2+}, Zn^{2+} and Cr^{6+}; particle size, 63μm Zn^{2+} and 75 μm for Fe^{2+}, Pb^{2+} and Cr^{6+}; adsorbent dose, 4.0 g/L for Fe^{2+}, Zn^{2+} and Cr^{6+} and 5.0 g/L for Pb^{2+}; agitation speed, 250 rpm for Cr^{6+} and 300 rpm for Fe^{2+}, Pb^{2+}, Zn^{2+}; temperature, 333 K for Fe^{2+}, 328K for Zn^{2+} and Pb^{2+} and 318K for Cr^{6+}; initial metal ion concentration, 100 mg/L.

Adsorption Kinetics
The adsorption data obtained for Fe^{2+}, Pb^{2+}, Zn^{2+}, and Cr^{6+} ions on AK-clay while studying the effect of temperature were analyzed using Pseudo first-order, Pseudo second-order, Elovich and Intra-particle particle diffusion kinetic models (Table 2). From the results, Pseudo second-order kinetic model best fit the data for adsorption of all the metal ions with regression coefficient (R^2) values of 0.9994, 0.9999, 0.9990 and 0.9989 for Fe^{2+}, Pb^{2+}, Zn^{2+}, and Cr^{6+} ions respectively at optimum temperature as a function of contact time (Figure 11). The kinetic model satisfactorily shows good

agreement between the experimental values of the adsorbed metal ions (q_{x-exp}) and the model predicted values (q_{x-cal}). From Elovich kinetic model, Cr^{6+} ion gave the highest constant β (0.935 g/mg); an Elovich constant related to the degree of surface coverage and activation energy (Wu *et al.*, 2009; Ramachandra *et al.*, 2011). A shown in Figure 12, the intra-particle diffusion plots for the metal ions are linear over the time range but do not pass through the origin. This implies that intra-particle diffusion is not the only rate-controlling step, but may have occur simultaneously with film diffusion process. Similar rate-controlling steps

for adsorption have been reported (Sen and Gomez, 2011; Nethaji *et al*., 2013). From the results, Fe^{2+} ion exhibited the highest initial rate of adsorption α (66.531 g.min^2/mg), while adsorption of Pb^{2+} ion presented the largest intercept value of 14.735. This indicates that Pb^{2+} ion adsorption has greater boundary layer thickness than other metal ions; large intercept corresponds to greater boundary layer effect (Bulut and Tez, 2007).

The results of pseudo second-order kinetic model shows the rate constant of adsorption increased as the temperature of Fe^{2+} and Zn^{2+} ions increased from 303-333 K, corresponding to increase in their uptake. Rate constant increased for Cr^{6+} and Pb^{2+} ions as the temperature increased from 303 to 323 and 328 K respectively. Further increase in temperature resulted in a decline in their rate constant, indicating that their adsorption on AK-

clay was less favourable at a temperature of 333 K and above. This agrees with similar findings in a recent report (Khansaa and Fawwaz, 2018).

The activation energy values were determined from the slope of lnk$_2$ against 1/T (Figure 13) in the Arrhenius equation ($lnk_2 = lnA - \dfrac{Ea}{RT}$), where, k$_2$ is second order rate constant and *Ea* is the activation energy (Adebowale *et al*., 2008). The *Ea* values obtained for Fe^{2+}, Pb^{2+}, Zn^{2+} and Cr^{6+} ions were 11.55, 13.52, 6.5 and 17.34 kJ /mol respectively. Since the *Ea* values are less than 40 kJ /mol, the mechanism of adsorption of the metal ions on AK-clay is physisorption. In physisorption process, *Ea* is lower than 40 kJ /mol while value greater than 40 kJ /mol signify chemisorption (Al-Ghouti *et al*., 2005; Inglezakis and Zorpas, 2012).
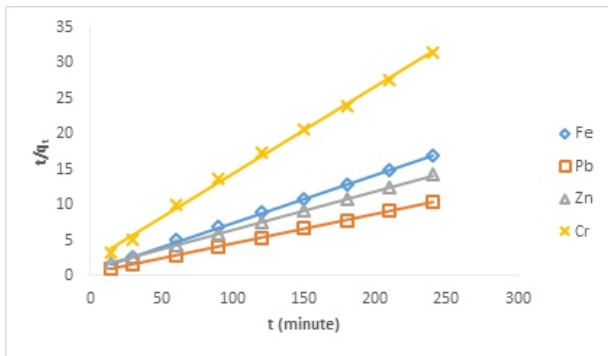

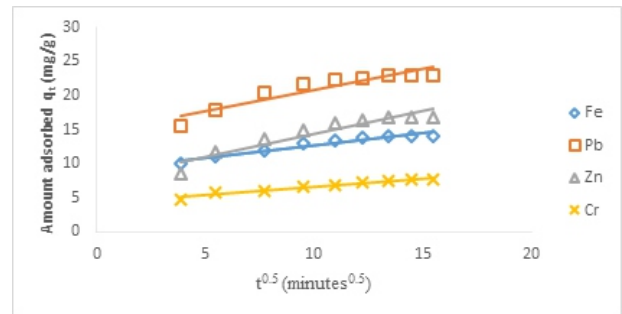Figure 11: Pseudo second-order kinetic model at optimum temperature

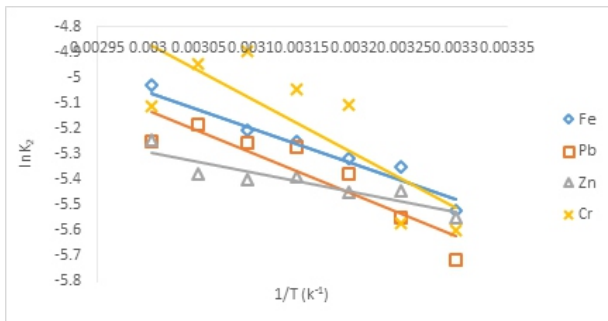Figure 12: Intra-particle diffusion kinetic model for the metal ions on AK-clay

Figure 13: Arrhenius plot for adsorption of metal ions on AK-clay

Table 2. Kinetic parameters at optimum temperature

Kinetic model	Parameter	Fe^{2+}	Pb^{2+}	Zn^{2+}	Cr^{6+}
	Temp. (K)	333	328	333	323
First-order	Relationship	y= -0.0059x + 0.5762	y= -0.0052x + 0.6811	y= -0.0053x + 0.7551	y= -0.0053x + 0.4567
	R^2	0.597	0.4785	0.555	0.5298
	K (min^{-1})	0.0140	0.012	0.012	0.012
	q_x (mg/g)	3.767	4.798	3.589	3.387
Second-order	Relationship	y= 0.068x + 0.7074	y = 0.0521x + 0.4867	y= 0.0565x +0.687	y= 0.1172x + 3.1194
	R^2	0.9994	0.9999	0.9990	0.9989
	q_{xcal} (mg/g)	14.706	19.134	17.639	8.532
	K (g/mg.min)	6.54×10^{-3}	5.61×10^{-3}	4.65×10^{-3}	4.4×10^{-3}
Elovich	Relationship	y= 1.5735x + 5.7293	y= 2.7562x + 8.6376	y= 3.0062x − 1.1343	y= 1.0297x + 1.8397
	R^2	0.9823	0.9651	0.9725	0.9780
	β (g/mg)	0.636	0.363	0.333	0.935
	α (mg/g.min)	66.531	63.259	4.379	0.935
Intra-particle diffusion	Relationship	y= 0.3579x + 9.1082	y= 0.6096x + 14.735	y= 0.6684x + 7.7494	y= 0.2462x + 4.1068
	R^2	0.9337	0.8674	0.8831	0.9517
	K ($mg/g.min^{-0.5}$)	0.3579	0.6096	0.6684	0.2462

Adsorption Isotherm Modeling of the Adsorption Data

The adsorption equilibrium data for Fe^{2+}, Pb^{2+}, Zn^{2+} and Cr^{6+} ions on AK-clay were analyzed using Langmuir, Freundlich, Tempkin, Dubinin-Radushkevich and Flory-Huggins isotherm models (Table 3). From the values of the correlation coefficient (R^2) obtained, Langmuir isotherm model best fitted the adsorption process for Fe^{2+}, Zn^{2+} and Cr^{6+} ion with R^2 values of 0.9923, 0.8873 and 0.9307 respectively, while Freundlich isotherm model best described the adsorption of Pb^{2+} ion with R^2 value of 0.9782 (Figure 14). From the Langmuir isotherm, adsorption of Pb^{2+} presented the highest monolayer adsorption capacity Q_o (40.812 mg/g) and the lowest binding energy constant (b) of 0.047 dm^3/mg. The Q_o values for Fe^{2+}, Zn^{2+} and Cr^{6+} are 13.66, 17.99 and 9.52 mg/g, while the binding energy constant (b) are 0.229, 0.068 and 0.055 dm^3/mg respectively. The Freundlich adsorption isotherm heterogeneity factor $1/n$, shows the adsorption of Fe^{2+} ion is more heterogeneous as its value is closer to zero than other metal ions (Foo and Hameed, 2010). However, the adsorption intensity for all the metal ions was considered favourable as all $1/n$ values were less than one (Fe^{2+}, 0.1443; Pb^{2+}, 0.59 Zn^{2+}, 0.23; Cr^{6+}, 0.156). Dubinn-Radushkevich (D-R) theoretical saturated capacity (q_A) of Pb^{2+} ion (1096.48 mg/g) was the highest and this confirms the Q_o value calculated using Langmuir isotherm model.
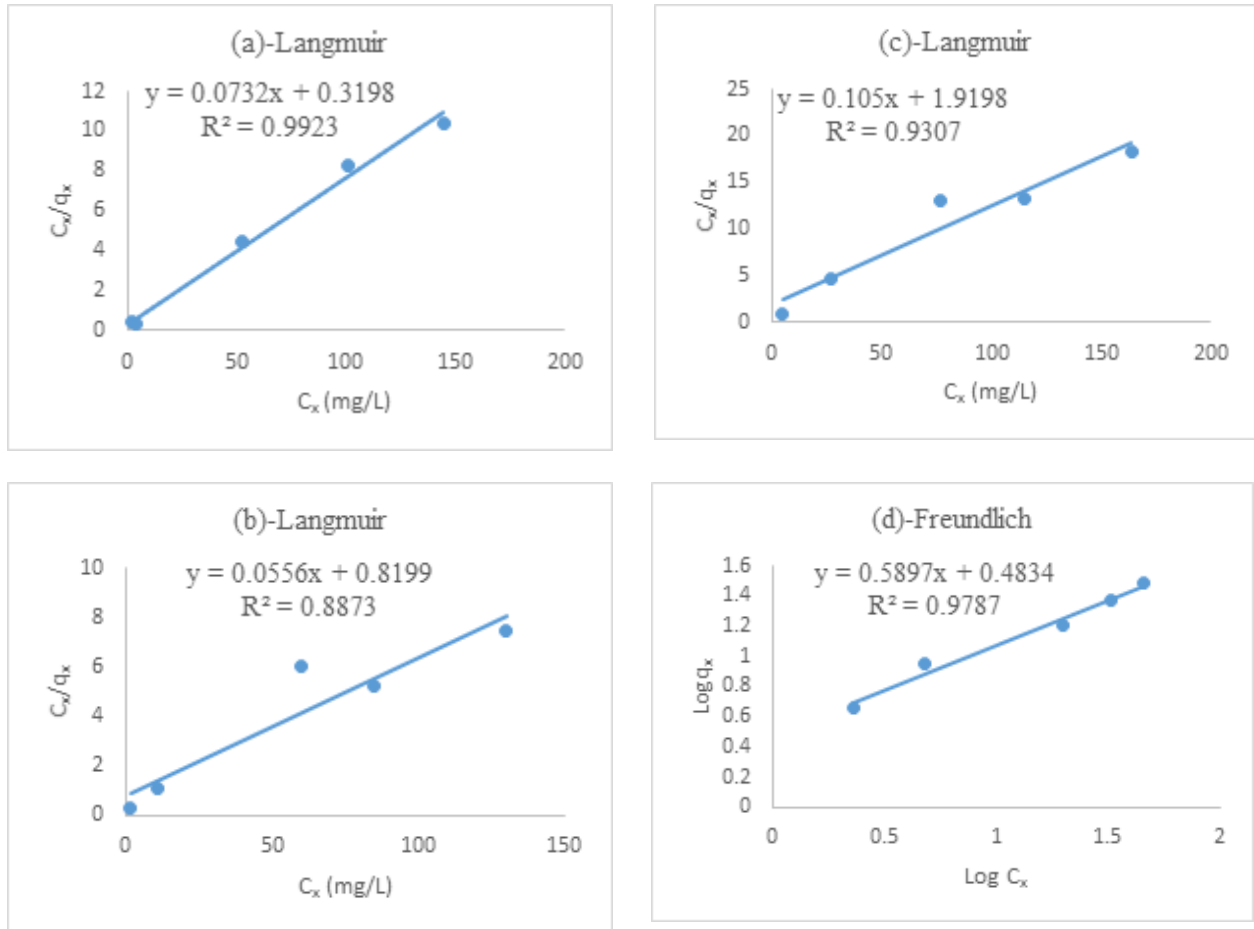
Figure 14: Adsorption isotherm model: (a) Fe^{2+} (b) Zn^{2+} (c) Cr^{6+} (d) Pb^{2+}

Table 3. Isotherm model parameters for adsorption of Fe^{2+}, Pb^{2+}, Zn^{2+} and Cr^{6+} ions on AK-clay

Isotherm model	Parameter	Fe^{2+}	Pb^{2+}	Zn^{2+}	Cr^{6+}
Langmuir	R^2	0.9923	0.8882	0.8873	0.9307
	Q_o (mg/g)	13.661	40.816	17.986	9.524
	b (dm^3/mg)	0.229	0.047	0.068	0.055
Freundlich	R^2	0.5908	0.9782	0.8579	0.7086
	$1/n$ (unitless)	0.1443	0.4834	0.7146	0.5669
	K_f (mg/g)	3.898	3.044	5.183	6.109
Tempkin	R^2	0.6386	0.9194	0.7802	0.6685
	A_T (L/g)	179.67	1.527	5.274	14.951
	b_T (J/mol)	1719.75	287.34	943.44	2155.67
Dubinin-Radushkevich (D-R)	R^2	0.8892	0.8349	0.6635	0.3712
	q_A (mg/g)	374.37	1096.48	373.08	94.04
	β (kJ^2 /mol^2)	1×10^{-06}	2.0×10^{-06}	7.0×10^{-07}	2.0×10^{-06}
Flory-Huggin	R^2	0.9011	0.9119	0.8102	0.8660
	K_F (L/mol)	1.3×10^{-03}	2.84×10^{-04}	184×10^{-03}	1.045×10^{-03}
	n (unitless)	0.062	0.012	0.062	6.02×10^{-03}
		-14.93	-18.54	-14.30	-15.58

Determination of Thermodynamic Parameters from Adsorption Data

The thermodynamic parameter results obtained for the adsorption on AK-clay showed that the $\Delta G°$ values of the metal ions were negative (Table 4). This indicates that the adsorption of the metal ions is spontaneous and thermodynamically feasible in the temperature range of 303 - 333K. $\Delta G°$ values of Fe^{2+}, Zn^{2+} and Cr^{6+} ions ranged between -15.41 to -19.13 kJ /mol, -15.39 to -20.88 kJ /mol and -13.24 to -15.67 kJ /mol respectively as the temperature increased from 300 to 333K. This shows increase in temperature favours their adsorption. Values of $\Delta G°$ for Pb^{2+} ranged between -22.15 to -27.77 kJ /mol as the temperature increased from 303 to 328K. Increasing the temperature to 333K resulted in lower negative values for $\Delta G°$ (-27.42 kJ /mol). This is an indication that the adsorption of Pb^{2+} ion is less favourable at 333 K. From the results, the decreasing order of the spontaneity of the adsorption of the metal ions is $Pb^{2+} > Zn^{2+} > Fe^{2+}$

> Cr^{6+} which corresponds to their adsorption capacity. Positive enthalpy ($\Delta H°$) values which implies endothermic process were obtained for all the metal ions in the following order: Pb^{2+}, 54.61 kJ /mol > Zn^{2+}, 42.03 kJ /mol > Fe^{2+}; 20.41 kJ /mol > Cr^{6+}, 6.21 kJ /mol. These value which are less than 80 kJ /mol, confirmed that their adsorption process is physisorption. In general, ΔH values lower than 80 kJ /mol indicate physisorption while heats of chemisorption is higher than 80 kJ /mol (Inglezakis and Zorpas, 2012). Positive values of $\Delta S°$ were obtained for the metal ions in the following order: Pb^{2+}, 248.35 $JK^{-1}mol^{-1}$ > Zn^{2+}, 188.42 $JK^{-1}mol^{-1}$ > Fe^{2+}, 118.96 $JK^{-1}mol^{-1}$ > Cr^{6+} 35.39 $JK^{-1}mol^{-1}$. The positive $\Delta S°$ value implies that there was some degree of randomness at the solid/liquid interface with Pb^{2+} ion recording the highest value. Similar values for thermodynamic parameters have been reported in literature (Adebowale *et al.*, 2008; Li *et al.*, 2010; Chai *et al.*, 2017).

Table 4. Thermodynamic parameters for adsorption of Fe^{2+}, Pb^{2+}, Zn^{2+} and Cr^{6+} on AK-clay

Temperature (K)		303	308	313	318	323	328	333
Fe^{2+}	$\Delta G°$ (kJ/mol)	-15.41	-16.28	-17.05	-17.55	-18.03	-18.49	-19.13
Pb^{2+}	$\Delta G°$ (kJ/mol)	-20.21	-22.15	-23.54	-24.20	-25.28	-27.77	-27.42
Zn^{2+}	$\Delta G°$ (kJ/mol)	-15.39	-15.94	-16.66	-17.60	-18.81	-19.91	-20.88
Cr^{6+}	$\Delta G°$ (kJ/mol)	-13.24	-13.58	-14.03	-14.63	-15.47	-15.51	-15.67
		Fe^{2+}	Pb^{2+}	Zn^{2+}	Cr^{6+}			
$\Delta H°$ (kJ/mol)		20.41	54.61	42.03	6.21			
$\Delta S°$ (J $mol^{-1}K^{-1}$)		118.96	248.35	188.42	35.39			

CONCLUSIONS

The 63 µm fraction of the purified Nigeria kaolinite clay obtained from Argungu deposit was found to contain kaolin as the only clay minerals present with high content of alumina and silica. The surface area parameters of the natural and modified clay is in the order of AK-AO clay > AK-clay > AK-S clay. The studied parameters investigated were found to influence the adsorption of Fe^{2+}, Pb^{2+}, Zn^{2+} and Cr^{6+} ions on the natural clay. The rate of uptake of the metal ions was in the order of $Pb^{2+} > Fe^{2+} > Zn^{2+} > Cr^{6+}$ ion. Modification of the clay with ammonium oxalate significantly increased the adsorption capacity for Fe^{2+} ion while using NaOH for the modification increased the capacity of the clay for all the metal ions. Statistical modeling of the experimental results based on ANOVA validated the

significance of the adsorption data with p-values < 0.001 at 95 % confidence limit and high F-values for all the metal ions. The adsorption equilibrium data obtained were best described with Langmuir isotherm model for Fe^{2+}, Zn^{2+} and Cr^{6+} ions and Freundlich isotherm model for Pb^{2+} ion respectively. Pseudo second-order kinetic model best explained the mechanism of the adsorption of the metal ions. The values of $\Delta G°$, $\Delta H°$ and $\Delta S°$ obtained for all the metal ions show the adsorption process is spontaneous, endothermic and entropy driven. The activation energy and $\Delta H°$ values obtained suggest physisorption as the mechanism of adsorption of the metal ions on AK-clay. From the results, AK-S clay increased the adsorption capacity for all the metal ions while AK-AO only improved the uptake of Fe^{2+} and Zn^{2+} ions.

REFERENCES

Adebowale, K.O., Unuabonah, E.I., Olu-Owola, B.I. (2008). Kinetics and thermodynamic aspects of the adsorption of Pb^{2+} and Cd^{2+} ions on tripolyphosphate-modified kaolinite clay. *Chemical Engineering Journal*, 136, 99-107.

Ajemba, R.O. (2014). Kinetics and equilibrium modeling of lead (II) and chromium (III) ions adsorption onto clay from Kono-bowe, Nigeria. *Turkish Journal of Engineering and Environmental Sciences.* 38, 455-479.

Al-Ghouti, M., Khraisheh, M.A.M., Ahmad, M.N.M. and Allen, S. (2005). Thermodynamic behavior and the effect of temperature on the removal of dyes from aqueous solution using modified diatomite: A kinetic study. *Journal of Colloid Interface Science*, 287, 6-13.

Al-Harahsheh, M., Shawabkeh, R., Al-Harahsheh, A., Tarawneh, K. and Batiha, M.M. (2009). Surface modification and characterization of Jordanian kaolinite: Application for lead removal from aqueous solutions. *Applied Surface Science*, 255, 8098-8103.

Aliabadi, M., Khazaei, I., Fakhraee, H. and Mousavian, M.T.H. (2012). Hexavalent chromium removal from aqueous solutions by using low-cost biological wastes: equilibrium and kinetic studies. *International Journal of Environmental Science and Technology*, 9(2), 319-326.

Anastopoulos, I. and Kyzas, G.Z. (2016). Are the thermodynamic parameters correctly estimated in liquid-phase adsorption phenomena? *Journal of Molecular Liquids*, 218, 174-185.

Arivoli, S., Marimuthu, V. and Jahangir, A.R.M. (2013). Kinetics of batch adsorption of iron (II) ions from aqueous solution using activated carbon from Strychnos Nux-Vomica L. *International Journal of Scientific & Engineering Research*, 4(12), 407-417.

Barth, N.E. (1994). Elementary crystallography and mineralogy. University of Calabar Press, Calabar, pp. 105-107.

Bergaya, F., Theng, B. and Lagaly, G. (2006). Handbook of Clay Science, Elsevier, Amsterdam, pp. 968-1103.

Bernard, E., Jimoh, A. and Odigure, J.O. (2013). Heavy metal removal from industrial wastewater by activated carbon prepared from Coconut shell. *Research Journal of Chemical Sciences,* 3(8), 3-9.

Bhattacharyya, K.G. and Gupta, S.S. (2008). Adsorption of a few heavy metals on natural and modified kaolinite and montmorillonite: A review. *Advances in Colloid and Interface Science,* 140, 114-131.

Bhattacharyya, K.G. and Gupta, S.S. (2011). Removal of Cu(II) by natural and acid-activated clays: An insight of adsorption isotherm, kinetic and thermodynamics. *Desalination*, 272, 66-75.

Bingol, D., Canbazoglu, M. and Aydogan, S. (2005). Dissolution kinetics of malachite in ammonia/ammonium carbonate leaching. *Hydrometallurgy*, 76, 55-62.

Biswas, S., Bal, M., Behera, S.K., Sen, T.K. and Meikap, B.C. (2019). Process optimization study of Zn^{2+} adsorption on biochar-alginate composite adsorbent by Response Surface Methodology (RSM). *Water*, 11, 325.

Bulut, Y. and Tez, Z. (2007). Removal of heavy metals from aqueous solution by sawdust adsorption. *Journal of Environmental Sciences*, 19, 160-166.

Chai, W., Huang, Y., Su, S., Han, G., Liu, J. and Yijun, C.A.O. (2017). Adsorption behavior of Zn(II) onto natural minerals in wastewater. A comparative study of bentonite and kaolinite. *Physicochemical Problems of Mineral Processing,* 53(1), 264-279.

Chandra, D. and Mandal, A.R. (2000). Toxicological and pharmacological study of Navbal Rasayan-A metal based formulation. *Indian Journal of Pharmacology*, 32, 36-42.

Cheng, T.W., Lee, M.L., Ko, S.M., Ueng, T.H. and Yang, S.F. (2012). The heavy metal adsorption characteristics on metakaolin-base geopolymer. *Applied Clay Science,* 56, 90-96.

Cruz-Guzman, M., Celis, R., Hermosin, M.C., Koskinen, W.C., Nater, E.A. and Cornejo, J. (2006). Heavy metal adsorption by Montmorillonites modified with natural organic cations. *Soil Science Society of America Journal,* 70, 215-221.

Das, B., Mondal, N.K. Bhaumik, R. and Roy, P. (2014). Insight into adsorption equilibrium, kinetics and thermodynamics of lead onto alluvial soil. *International Journal of Environmental Science and Technology*, 11, 1101-1114.

Dawodu, F.A. and Akpomie, K.G. (2014). Simultaneous adsorption of Ni(II) and Mn(II) ions from aqueous solution unto a Nigerian kaolinite clay. *Journal of Material Research and Technology*, 3(2), 129-141.

Djomgoue, P. and Njopwouo, D. (2013). FT-IR spectroscopy applied for surface clays, *Journal of Surface Engineered Materials and Advanced Technology,* 3, 275-28.

Donat, R., Akdogan, A., Erdem, E. and Cetisli. H. (2005). Thermodynamics of Pb2+ and Ni2+ adsorption onto natural bentonite from aqueous solutions. *Journal of Colloid and Interface Science*, 286, 43-52.

Doss, V.R. and Kodolikar, S.P. (2012). Heavy metal adsorption by ligand granular activated carbon: Thermodynamics and Kinetics. *International Journal of Chemical Engineering and Applications,* 5(2): 88-95.

Emam, A.A., Ismaila, L.F.M. and AbdelKhalekb, M.A. (2016). Adsorption study of some heavy metal ions on modified kaolinite clay. *International Journal of Advancement in Engineering Technology, Management and Applied Science*, 3(7), 152-163.

Fakoluji, O.S., Olokode, O.S., Aiyedun, P. O., Oyeleke, Y.T., Anyanwu, B.U. and Lee, W.E. (2012). Studies on the five selected clays in Abeokuta, Nigeria. *The Pacific Journal of Science and Technology,* 13(1), 83-90.

Fan, Y, Zhang, C., Wu, J., Zhan, J. and Yang, P. (2010). Composition and morphology of complicated copper oxalate powder. *Transaction Nonferrous Metals Society China*, 20,165-170.

Foo, K.Y. and Hameed, B.H. (2010). Insights into the modeling of adsorption isotherm systems. *The Chemical Engineering Journal,* 156(1), 2-10.

Griffin, R.A. Anna, K.A. and Frost, R.R. (1977). Effect of pH on adsorption of chromium from landfill-leachate by clay minerals. Journal of Environmental Science and Health. Part A: Environmental Science and Engineering: *Toxic/Hazardous Substances and Environmental Engineering,* 12(8), 431-449.

Ho, Y.S. (2004). Citation review of Lagergren kinetics rate equation on adsorption reactions. *Scientometric,* 59, 171-177.

Inglezakis, V. J., and Zorpas, A. A. (2012). Heat of adsorption, adsorption energy and activation energy in adsorption and ion exchange systems. *Desalination and Water Treatment,* 39(1-3), 149-157.

Itodo, A.U. and Itodo, H U. (2010). Sorption energies estimation using Dubinin-Radushkevich and Tempkin adsorption isotherms. *Life Science Journal,* 7(4), 31-39.

Jiang, M., Jin, X., Lu, X. and Chen, Z. (2010). Adsorption of Pb(II), Cd(II), Ni(II) and Cu(II) onto natural kaolinite clay. *Desalination*, 252, 33-39.

Jiang, M., Wang, Q., Jin, X. and Chen, Z. (2009). Removal of Pb(II) from aqueous solution using modified and unmodified kaolinite clay. *Journal of Hazardous Materials*, 170(1), 332-339.

Kalantari, K., Ahmad, M. B., Fard-Masoumi, H. R., Shameli, K., Basri, M. and Khandanlou, R. (2014). Rapid and high capacity adsorption of heavy metals by Fe_3O_4/montmorillonite nanocomposite using response surface methodology: Preparation, characterization, optimization, equilibrium isotherms, and adsorption kinetics study. *Journal of the Taiwan Institute of Chemical Engineers*, 49, 192-198.

Kamel, M.M., Ibrahim, M.A., Ismael, A.M. and El-Motaleeb, M.A. (2004). Adsorption of some heavy metal ions form aqueous solutions by using kaolinite clay. *Assiut University Bulletin of Environmental Research,* 7(1), 101-109.

Khansaa, A. and Fawwaz, K. (2018). Heavy metals adsorption from aqueous solutions onto unmodified and modified Jordanian kaolinite clay: batch and column. Techniques. *American Journal of Applied Chemistry.* 6(1), 25-34.

Kooli, F., Hian, P.C., · Weirong, Q., Alshahateet, S.F. and Chen, F. (2006). Effect of the acid-activated clays on the properties of porous clay hetero-structures. *Journal of*

Porous Mater, 13, 319-324.

Krishna, B.S., Murthy, D.S.R. and Prakash, B.S. (2001). Surfactant-modified clay as adsorbent for chromate. *Applied Clay Science*, 20, 65-71.

Lee, M.H., Kim, C.J. and Boo, B.H. (2000). Electrodeposition of alpha-emitting nuclides from ammonium oxalate-ammonium sulfate electrolyte. *Bulletin of Korean Chemical Society*, 21(2), 175-179.

Lee, S.M. and Tiwari, D. (2012). Organo and inorgano-organo-modified clays in the remediation of aqueous solutions: An overview. *Applied Clay Science*, 59-60, 84-102.

Li, Y., Yue, Q.Y. and Gao, B.Y. (2010). Effect of humic acid on the Cr(VI) adsorption onto Kaolin. *Applied Clay Science*, 48(3), 481-484.

Liu, Y. (2009). Is the free energy change of adsorption correctly calculated? *Journal of Chemical Engineering Data*, 54, 1981-1985.

Mahmoud, M. A. (2015). Kinetics and thermodynamics of aluminum oxide Nano powder as adsorbent for Fe (III) from aqueous solution. *Beni-Suef University Journal of Basic and Applied Sciences,* 4(2), 142-149.

Meroufel, B., Benali, O., Benyahia, M., Zenasni, M.A., Merlin, A. and George, B. (2013). Removal of Zn (II) from aqueous solution onto kaolin by batch design. *Journal of Water Resource and Protection*, 5, 669-680.

Mielniczek-Brzohska, E., Giezak-KocHwin, K. and Sangwal, K. (2000). Effect of Cu (II) ions on the growth of ammonium oxalate monohydrate crystals from aqueous solutions: growth kinetics, segregation coefficient and characterization of incorporation sites. *Journal of Crystal Growth*, 212, 532-542.

Nethaji, S., Sivasamy, A. and Mandal, A.B. (2013). Adsorption isotherms, kinetics and mechanism for the adsorption of cationic and anionic dyes onto carbonaceous particles prepared from *Juglans regia* shell biomass. *International Journal of Environmental Science and Technology*, 10, 231-242.

Olaofe, O., Olagboye, S.A. Akanji, P.S. Adamolugbe, E.Y., Fowowe, O.T. and Olaniyi, A.A. (2015). Kinetic studies of adsorption of heavy metals on clays. *International Journal of Chemistry*, 7(1), 48-54.

Olokode, O.S., Aiyedun, P.O., Kuye, S.I., Adekunle, N.O. and Lee, W.E. (2010). Evaluation of a clay mineral deposit in Abeokuta, South-West Nigeria. *Journal of Natural Sciences, Engineering and Technology,* 9(1), 132-136.

Olusola, J.O., Suray, A.A., Temitope, M.A. and Aminat, O.A (2011). Sedimentological and geochemical studies of Maastrichtian clays in Bida Basin, Nigeria: Implication for resource potential. *Centre Point Journal (Science Edition),* 17(2), 71-88.

Osabor, V. N., Okafor, P. C., Ibe, K. A. and Ayi, A. A. (2009). Characterization of clays in Odukpani, south eastern Nigeria. *African Journal of Pure and Applied Chemistry,* 3(5): 79-85.

Panda, A.K., Mishra, B.G. Mishra, D.K. and Singh, R.K. (2013). Effect of sulphuric acid treatment on the physico-chemical characteristics of kaolin clay. *Colloids and Surfaces* A: Physicochemical and Engineering Aspects, 363, 98-104.

Qiao, Y., Wang, K., Yuang, H., Yang, K. and Zou, B. (2015). Negative linear compressibility in organic mineral ammonium oxalate monohydrate with hydrogen bonding wine-rack motifs. *Journal of Physical Chemistry Letters*, 6, 2755-2760.

Ramachandran, P., Vairamuthu, R. and Ponnusamy, S. (2011). Adsorption isotherms, kinetics, thermodynamics and desorption studies of reactive orange16 on activated carbon derived from A*nanas comosus* (L.) CARBON. *ARPN Journal of Engineering and Applied Sciences*, 6(11), 15-26.

Rane, N.M. and Sapkal, R.S. (2014). Chromium (VI) removal by using orange peel powder in batch adsorption, *International Journal of Chemical Sciences and Applications*, 5(2), 2014, 22-29.

Sari, A., Tuzen, M., Citak, D. and Soylak, M. (2007). Equilibrium, kinetic and thermodynamic studies of adsorption of Pb(II) from aqueous solution onto Turkish kaolinite clay. *Journal of Hazardous*

Materials, 149(2), 283-291.

Sen, T.K. and Gomez, D. (2011). Adsorption of zinc (Zn^{2+}) from aqueous solution on natural bentonite. *Desalination*, 267, 286-294.

Stoppe, N., Amelung, W., Horn, R. (2015). Chemical extraction of sedimentary iron oxy(hydroxides) using ammonium oxalate and sodium dithionite revisited – an explanation of processes in coastal sediments. *Agro Sur,* 43(2), 11-17.

Subramanyam, B. and Ashutosh, D. (2012). Adsorption isotherm modeling of phenol onto natural soil: Application of various isotherm models. *International Journal of Environmental Research,* 6(1), 265-276.

Theivarsu, C. and Mylsamy, S. (2011). Removal of Malachite green from aqueous solution by activated carbon developed from cocoa (*Theobroma Cacao*) shell-A kinetic and equilibrium studies. *E-Journal of Chemistry,* 8(S1), S363-S371.

Uddin, M.K. (2017). A review on the adsorption of heavy metals by clay minerals, with special focus on the past decade. *Chemical Engineering Journal*, 308, 438-462.

Vaculikova, L. and Plevora, E. (2005). Identification of clay minerals and micas in sedimentary rocks. *Acta Geodynamics Geomaterials*, 2(2), 163-171.

Wu, C., Tseng, R. and Juang, R. (2009). Characteristics of Elovich equation used for the analysis of adsorption kinetics in dye-chitosan systems. *Chemical Engineering Journal*, 150, 366-373.

Xi, Y., Mallavarapu, M. and Naidu, R. (2010). Preparation, characterization of surfactants modified clay minerals and nitrate adsorption. *Applied Clay Science*, 48, 92-96.

Zhou, X and Zhou, X. (2014). The unit problem in the thermodynamic calculation of adsorption using the Langmuir equation. *Chemical Engineering Communication*, 201, 1459-1467.

Zhu, X., Zhu, Z., Lei, X. and Yan, C. (2016). Defects in structure as the sources of the surface charges of kaolinite. *Applied Clay Science*, 124-125, 127-1363.